Mechanical modelling of the axial behaviour of traditional masonry wall metal tie connections in cavity walls

Arslan, O.; Messali, F.; Smyrou, E.; Bal, İ.E.; Rots, J.G.

DOI
10.1016/j.conbuildmat.2021.125205

Publication date
2021

Document Version
Final published version

Published in
Construction and Building Materials

Citation (APA)
Arslan, O., Messali, F., Smyrou, E., Bal, İ. E., & Rots, J. G. (2021). Mechanical modelling of the axial behaviour of traditional masonry wall metal tie connections in cavity walls. *Construction and Building Materials*, *310*, 1-13. Article 125205. https://doi.org/10.1016/j.conbuildmat.2021.125205

Construction and Building Materials 310 (2021) 125205

Contents lists available at ScienceDirect

Construction and Building Materials

journal homepage: www.elsevier.com/locate/conbuildmat

Mechanical modelling of the axial behaviour of traditional masonry wall metal tie connections in cavity walls

O. Arslan [a,b,*], F. Messali [b], E. Smyrou [a], İ.E. Bal [a], J.G. Rots [b]

[a] Research Centre for Built Environment NoorderRuimte, Hanze University of Applied Sciences, Groningen, the Netherlands
[b] Faculty of Civil Engineering and Geosciences, Delft University of Technology, Delft, the Netherlands

ARTICLE INFO

Keywords:
Unreinforced masonry
Existing brick masonry structures
Cavity walls
Wall ties
Mechanical model
Parametric analysis

ABSTRACT

The seismic assessment of unreinforced masonry (URM) buildings with cavity walls is a relevant issue in many countries, such as in Central and Northern Europe, Australia, New Zealand, China and several other countries. A cavity wall consists of two separate parallel masonry walls (called leaves) connected by metal ties: an inner loadbearing wall and an outer veneer having mostly aesthetic and insulating functions. Cavity walls are particularly vulnerable structural elements. If the two leaves of the cavity wall are not properly connected, their out-of-plane strength may be significantly smaller than that of an equivalent solid wall with the same thickness.

The research presented in this paper focuses on a mechanical model developed to predict the failure mode and the strength capacity of metal tie connections in masonry cavity walls. The model considers six possible failures, namely tie failure, cone break-out failure, pull-out failure, buckling failure, piercing failure and punching failure. Tie failure is a predictable quantity when the possible failure modes can be captured. The mechanical model for the ties has been validated against the outcomes of an experimental campaign conducted earlier by the authors. The mechanical model is able to capture the mean peak force and the failure mode obtained from the tests. The mechanical model can be easily adopted by practising engineers who aim to model the wall ties accurately in order to assess the strength and behaviour of the structures against earthquakes. Furthermore, the proposed mechanical model is used to extrapolate the experimental results to untested configurations, by performing parametric analyses on key parameters including a higher strength mortar of the calcium silicate brick masonry, a different cavity depth, a different tie embedment depth, and solid versus perforated clay bricks.

1. Introduction

Cavity wall is a construction practice that usually is used for thermal and weather resistance, and provide drainage as well [1,2]. Cavity walls are widely used for unreinforced masonry structures in many countries all over the world, especially for residential constructions. In the Netherlands, a cavity wall usually consists of an inner load-bearing wall made of calcium silicate brick masonry and an outer veneer of clay brick masonry separated by a cavity. Metal ties are used for connecting the inner load-bearing leaf to the outer veneer. However, large differences exist in the way a cavity wall is constructed around the world. Cavity walls that consist of an outer load-bearing leaf and an inner non-load-bearing leaf, opposite of the usual the practice in the Netherlands, can also be found [3]. Despite the advantages of cavity walls in terms of durability and installation functions such as humidity and moisture control, observations from damaged buildings have shown that cavity walls are vulnerable to out-of-plane failures when the connections between the two leaves are weak.

The behaviour of the cavity wall tie needs to be adequately investigated to be properly modelled (either analytically or numerically). For this reason an experimental campaign was conducted at the Delft University of Technology to provide benchmarks for the validation of analytical models for cavity wall ties [4]. The campaign was based on tests at the component level, including a large number of variations, such as two embedment lengths, four pre-compression levels, two different tie geometries, and five different testing protocols. The experimental campaign aimed to define the capacity of the cavity wall ties. Besides, different failure modes of the ties were observed during the

* Corresponding author at: Research Centre for Built Environment NoorderRuimte, Hanze University of Applied Sciences, Zernikeplein 11 9747AS, Groningen, the Netherlands
E-mail addresses: o.arslan@pl.hanze.nl (O. Arslan), F.Messali@tudelft.nl (F. Messali), e.smyrou@pl.hanze.nl (E. Smyrou), i.e.bal@pl.hanze.nl (İ.E. Bal), J.G.Rots@tudelft.nl (J.G. Rots).

https://doi.org/10.1016/j.conbuildmat.2021.125205
Received 21 June 2021; Received in revised form 3 October 2021; Accepted 6 October 2021

experimental campaign: namely sliding failure, tie failure, buckling failure and expulsion failure [4].

In the literature, various failure modes were reported for cavity wall tie connections either through tests at component level [5–8] or on full scale structures [9–13]. In the latter case, the primary cause of failure for most of cavity walls was related to the failure of the wall tie connections [7,12,13], rising the need of providing a better mechanical modelling for this structural component. Different types and geometries of the ties, errors in construction, insufficient embedment, and installation methods can affect the overall strength and failure modes of the tie connection. Nevertheless, little research (such as [14–17]) has been performed to define a mechanical model of cavity wall ties in masonry structures. On the other hand, the possible failure modes of anchors embedded in masonry bed joint are similar to those observed for cast-in-place headed anchors embedded in concrete, which have been widely studied under a variety conditions, such as for a single anchor far from edges [18–21] or for an anchor near edges [22,23].

Arifovic and Nielsen [24] too proposed an analytical model for anchors in masonry based on the theory of plasticity and calibrated after the experimental results conducted by Hansen et al. [25]. The proposed model was based on the distinction between local and global failure modes. The local failure modes regard the inner interface between the grout and the anchor, whereas the global failure modes regard the outer interface between masonry and grout. A total of five failure modes (combined brick-cone failure, splitting failure, sliding failure of an anchor in the joint and the brick, and punching failure) were defined in order to compute the load carrying capacity of the anchors. The proposed model in masonry was developed by analogy of the approach of the anchorage theory and it is worthy noticing that mortar can behave similarly to normal concrete [26].

Different failure modes of anchors in masonry walls are identified also by the Masonry Standards Joint Committee [27], such as rupture failure, pull-out failure and tensile cone break-out failure. A 45-degree cone model is used for predicting tensile cone break-out failure with a constant tensile stress acting over the projected failure cone by MSJC. However, MSJC does not take into account the difference between zigzag-end of the tie embedded in clay brick and hook-end of the tie embedded in calcium silicate, which is often present in constructions.

In compression, punching failure is a possible failure mode. Moe [28] proposed an empirical equation to compute the punching strength based on the experiments conducted by the author. In this proposed equation, the punching strength is proportional to the square root of the compressive strength of the concrete. The work of Moe served as a basis of punching shear design provisions of the ACI Building Code. The assessment of the punching failure is presented in the ACI 318–14 Building Code provisions [29] .

Lintz and Toubia [30] proposed a simplified analytical method to determine the amount of load transferred via the ties to the brick in veneers and found that placing vertical reinforcement in the outer leaves may allow for an increase of the design strength.

The metal ties studied in this paper are not initially designed and built against seismic forces. This is because Groningen was not a seismically prone area until recently when the gas extraction caused small shallow earthquakes. This is the reason why the metal ties studied may lack the necessary strength and ductility to resist the seismic actions. If designed and constructed properly, however, metal ties can make a significant contribution to the seismic resistance of masonry cavity walls. In the Australian practice, for example, several types of metal ties can be used in accordance with the Australian Masonry Structures Code, AS 3700 [31]. An extensive research supports this, for example Page et al. [32] developed an analytical model to predict loads in the wall ties under seismic actions. The study provides a valuable understanding of the behaviour of cavity walls in terms of the relative stiffness and the boundary conditions of each leaf, and the stiffness of the ties. Another study was conducted on typical Australian cavity walls to determine individual tie forces subjected to lateral loads [33]. In this study, a steel strip tie was used between the outer and inner leaves. The strip ties are more flexible, and thus may fail in buckling at a very low load, compared to the L-shaped ties studied in this paper. A simplified test method was developed in order to monitor each individual tie force in the cavity wall so that tie force redistribution can be detected when cavity wall tie connections reach their capacity.

Considering the models already described in the literature and the outcomes of the experimental campaign carried out at the Delft University of Technology, a mechanical model which considers six different possible failure modes is proposed in this paper to define the axial behaviour of metal tie connections in masonry cavity walls. The outcomes of this research are limited to masonry walls with the characteristics considered, whereas other constructive techniques and/or materials would require specific studies. Namely, the mechanical model refers to connections in cavity walls made with calcium silicate bricks (CS) and solid or perforated clay bricks (CB). The model has been calibrated and validated against the experiments conducted by the authors carried out on the cavity wall tie at the Delft University of Technology. Finally, the proposed mechanical model has been used to integrate the outcomes of the experimental campaign by performing parametric analyses in order to assess the influence of several key parameters.

2. Possible failure modes of a cavity wall tie under axial loading

Metal ties are used in masonry buildings to connect the inner leaf made of CS brick masonry and outer ~~leaves~~ veneer of clay brick masonry in a cavity wall. Different types of cavity wall metal ties can be found. The current study focuses on cavity walls made of calcium silicate brick masonry (for the inner-leaf) and perforated clay brick masonry (for the outer leaf), connected by metal ties with a zigzag-end embedded in calcium silicate brick masonry (CS) and a hooked-end were embedded in perforated clay brick masonry (CB). The study presented here focuses on the axial behaviour of the cavity wall tie connections since the stiffness of the ties in shear is low, its capacity is limited and is usually neglected. In the following, the behaviour of the connections under tensile and compressive axial loads is distinguished. In the literature, pull-out failure and buckling failure are the common observed failure modes [4,5,34,35]. In total, six basic failure modes are identified.

When cavity walls are subjected to tensile loading, cavity wall ties may exhibit one of the following possible failure modes:

- Tie Failure: the yielding of the tie is followed by its fracture (Fig. 2a);
- Cone break-out failure: a cone-shaped portion of mortar around the tie detaches from the rest of the joint (Fig. 2b);
- Pull-out failure: the tie slides along the tie-mortar interface (Fig. 2c).

The failure of the tie is identified as an upper limit on the achievable load-carrying capacity of a metal tie. In order to detect tie failure in cavity walls, the outer interface between the mortar of the bed-joint and the bricks, as well as the inner interface between the tie and the mortar must provide adequate bond so that the tie will develop its yield strength.

The failure of the outer interface between the mortar joint and the brick can be described as a cone-shaped mortar breakout radiating outward from the base of the embedded tie. This failure can be seen in analogy with the cone failure in concrete [36]. It is assumed that the angle of the cone envelope is approximately 45-degrees with respect to the surface of the cavity walls. The failure mode can be described as composed of two contributions which are the cone break-out failure in the mortar and the shear failure along the both the interfaces between the mortar and the bricks.

Pull-out failure occurs due to poor bonding along the inner interface between the tie and the mortar. Therefore, the pull-out failure is characterized by an extensive slip of the tie, whereby the surrounding mortar does not have a significant splitting or crushing. The pull-out failure may govern the failure when the mechanical interlock is inadequate, and

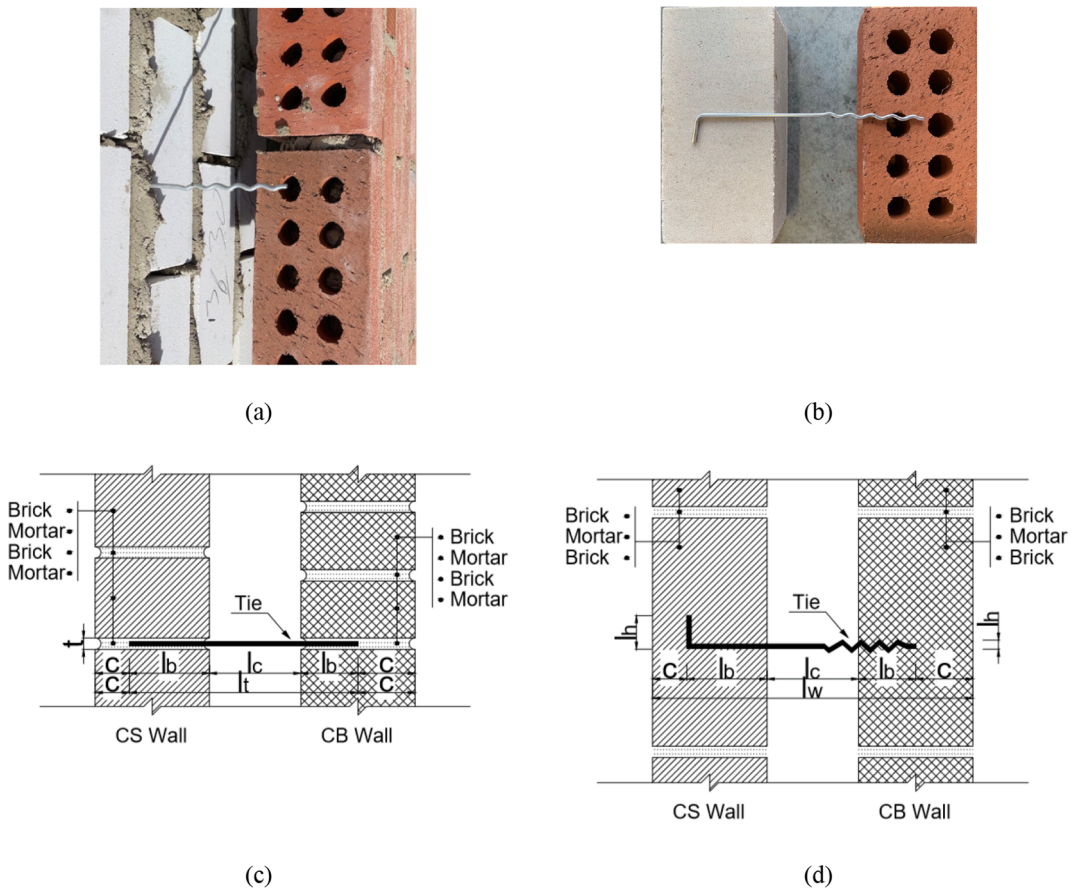

Fig. 1. View of cavity walls: tie embedded in CS(a), cavity wall tie(b), cavity wall side view (c) and cavity wall plan view (d).

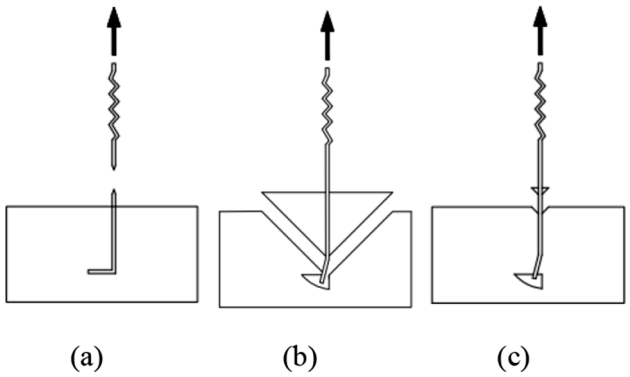

Fig. 2. Failure modes in Tension: Tie failure(a), Cone break-out failure (b) and pull-out failure (c).

thus it cannot develop sufficient frictional resistance in the inner interface.

Regarding the compressive loading, the cavity wall ties may exhibit one of the following failure modes:

- Buckling failure: the failure is caused by buckling of the tie (Fig. 4a);
- Piercing failure: the failure is achieved by piercing of the tie through the mortar (Fig. 4b);
- Punching failure: the failure is achieved by expulsion of the cone of mortar (Fig. 4c).

The failure of a cavity wall tie may be initiated by the buckling of the tie due to its initial imperfections, or a non-axial load. The buckling capacity of a metal tie can be simply computed via the Euler formula. The effective length factor may be chosen as 0.5 because the embedment in the mortar joints prevents rotations and translations at the two ends of the tie. In an earlier experimental work by Arslan et al. [3], it was found that bent ties, which often are observed in the practice due to the misalignment of the mortar joints, did not return significantly different performance compared to straight ties, and namely the buckling load was not affected.

The piercing failure of the cavity wall tie resembles closely the bearing failure of rigid plates in unreinforced concrete, for which Hawkins [37] proposed a mechanical model. In his approach, a wedge forms underneath the bearing plate and splits the surrounding concrete as it is pushed downward. Similarly, the piercing failure of cavity wall ties can be characterized by a cone of mortar radiating underneath from the base of the tie, and the slope of the piercing envelope with respect to the surface of the mortar joint is approximately 90-degree.

One of the most common failure that can be seen in concrete is punching shear of slabs. The punching failure can be defined as a possible failure mode for cavity wall ties as well [24]. The punching failure of cavity wall ties can occur underneath the base of the embedded tie in the mortar joint. Thus, the approach suggested by ACI for concrete can be applied also for computing the punching capacity of metal ties in cavity wall; as a result, traditional analytical procedure to determine the punching shear strength of unreinforced concrete slabs can be followed.

Although not observed in the experiments by Arslan et al. [4], a combination of failure modes may also occur in some cases. One of the reasons why such a combination was not captured experimentally may be the fact that, once a failure mode is activated, localization of damage accelerates the development of that failure mode.

3. The mechanical model for a wall tie connection

A mechanical model is proposed in the following sections for each of the six basic failure modes presented in the previous section. Once the strength of each mechanism is known, the dominant failure mode is then derived by assuming that the failure with the lowest strength governs the capacity of the connection.

The geometry used to define the model is shown in Fig. 1. The cavity walls analysed in this paper consist of an inner loadbearing leaf which is composed of calcium silicate bricks and an outer veneer made with clay bricks. L-shaped cavity wall ties with diameter 'd' and total length 'l_t' are embedded between two bricks in the mortar joint with thickness 't'. Embedment length 'l_b' is different at each end of the tie in the leaves of cavity walls. The zigzag-end with length 'l_h' approximately two times of the diameter of the tie is embedded in the CB masonry, while the L hook-end with length 'l_h' is embedded in the inner CS walls. The cross section of the wall is shown in Fig. 1.c, while Fig. 1.d shows the plan view.

3.1. Tensile capacity of the connection

Cavity wall ties can transfer the applied tensile load to the masonry in a variety of forms. Load-transfer mechanisms may be typically identified by bonding, friction, straightening of the hooked end or of the zig-zag end (depending on the embedment of the tie). Three potential failure modes are identified: tie failure, cone break-out failure and pull-out failure. A sketch which depicts each proposed failure mode is shown in Fig. 2.

3.1.1. Tie failure

Tie failure occurs when the fracture strength of the steel is reached, while the mortar remains undamaged (Fig. 2a). Hence, the tie failure can occur when any failure of the interface between the tie and the mortar or of the mortar is prevented. For this reason, in order for the tie failure to occur the embedment depth of the tie needs to be deep, and the bond strength of mortar should be sufficiently large. The tensile strength of the tie determines then the strength of the connection. The nominal strength of the tie is calculated by using Eq. (1):

$$N = A_s \times f_u \tag{1}$$

where A_s is the area of the cross-section and f_u is the ultimate tensile strength of the tie. The tie failure represents the upper limit of the achievable tensile load-carrying capacity of a cavity wall tie connection.

3.1.2. Cone break-out failure

Cone break-out failure in masonry is a cone-like failure which is assumed to occur similarly to the corresponding mechanism in concrete. The failure mode is characterized by the formation of a prism of mortar radiating out from the embedded head of the tie. It is assumed that the prism has a failure angle of approximately 45-degrees and a constant tensile stress uniformly distributed over the projected area of the failure surface.

Using this approach, which was also incorporated into MSJC [27], the tensile break-out capacity of a single anchor can be calculated as follows:

$$N = 0.332 \times \sqrt{f_m} \times A_{pt} \tag{2}$$

where $0.332 \times \sqrt{f_m}$ represents the constant tensile stress and A_{pt} is the projected break-out area. Development of the projected break-out area of a single cavity wall tie may be restricted by the thickness of the mortar joint which is a limited space between the bricks. Therefore, this approach cannot be applied directly for the cavity wall ties which are embedded in mortar joint. The reduced projected tension area can be calculated by using Eq. (3):

$$A_{pt} = 2 \times l_b \times t + l_b^2 \left(\frac{\pi \times \theta}{180} - sin\theta \right) \tag{3}$$

with:

$$\theta = 2 \times arcsin\left(\frac{t/2}{l_b} \right) \tag{4}$$

where t is thickness of the mortar joint, l_b is the embedment length of the tie. In addition to the failure load predicted by Eq. (2), an additional contribution given by the friction at the interface between the mortar and the brick needs to be considered. Therefore, the contribution of the initial shear strength and the coefficient of friction of mortar needs to be taken into account on the interface of mortar and brick.

The revised equation is presented as Eq. (5), where the first term defines the tensile break out of the mortar, whereas the second and third term are related to the friction coefficient and the initial shear strength of mortar, respectively.

$$N = 0.332 \times A_{pt} \times \sqrt{f_m} + 2\left(\mu \times f_p + f_{v0}\right) \times A_w \tag{5}$$

where A_w is the effective area of the cone of the mortar (Fig. 3), μ is the coefficient of friction, f_{vo} is initial shear strength of mortar and f_p is precompression level acting orthogonally to the interface.

The initial shear strength and coefficient of friction vary for different masonry typologies. It should be noted that the initial strength of the perforated clay masonry can be much higher than CS or solid clay masonry due to the dowel effect [38].

3.1.3. Pull-out failure

The pull-out failure is characterised by the straightening of the tie, due to a combination of local crushing of mortar and the yielding of the tie, followed by extensive slip.

Kuhn and Shaikh [36] proposed a method for determining the pull-out strength of hooked anchors embedded in concrete and masonry construction which was also defined in MSJC. In their study, bond strength between the hooked anchor and masonry is neglected, while friction is included. The equation by Kuhn and Shaikh is revised with a semi-empirical relationship to be adopted for metal ties embedded in masonry, considering different tie geometries (hooked end, zig-zag end, bent), mortar (mortar between CS bricks or CB bricks) and types of bricks. The model is based on the sum of two components: a bearing force and a friction force. The pull-out strength for the hooked part of the tie embedment in the CS can be computed by using Eq. (6):

$$N = 1.5 \times f_m \times l_h \times d + \alpha \times \sqrt{f_m} \times \pi \times (l_h + l_b) \times d + \frac{12 \times E \times I \times \phi}{l_c \times d^3} \tag{6}$$

where $\emptyset$ is bending of the tie in radians in case of a bent tie. The first part of the expression of the equation refers to the bearing of the hooked anchor embedded in CS. The second term represents the frictional resistance and is computed by the surface area of the tie multiplied by a modification factor α calibrated against the experimental results leading to a semi-empirical relationship, whose value is chosen equal to 0.5 for

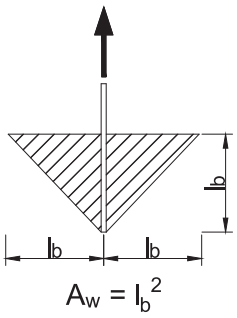

Fig. 3. Effective area of the cone of the mortar joint for shear strength.

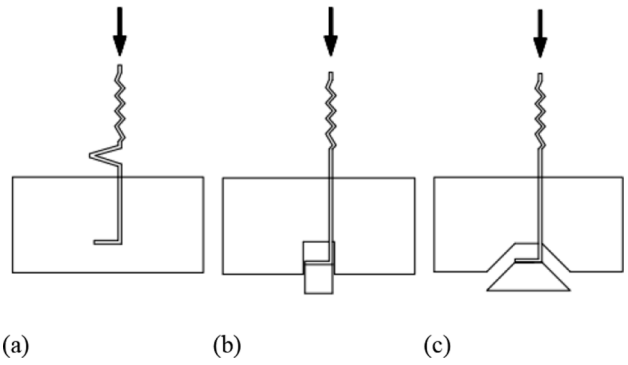

Fig. 4. Failure modes in Compression: Buckling failure(a), Piercing failure (b), Punching failure (c).

CS masonry. The last term represents the force needed to deflect the hooked end of the tie.

The pull-out strength for CB brick can be computed using Eq. (7):

$$N = 1.5 \times f_m \times l_b \times d + \alpha \times \sqrt{f_m} \times \pi \times l_b \times d \tag{7}$$

where α is a modification factor calibrated against the experimental results, whose value is chosen equal to 1 for CB masonry. A conservative value has been chosen for the modification factor since the shape of tie where embedded in mortar is zigzag representing thus deformed bar condition.

Different equations for computing the pull-out strength of CS and CB are needed due to the differences in behaviour of the embedded ends of the tie. The hooked part of the tie embedded in CS masonry is straightening due to the pull-out of the tie, while the zig-zag end of the tie embedded in CB masonry does not need to straighten.

3.2. Failure modes in compression

The failure modes of cavity wall ties in compression are classified into the following categories: buckling failure, punching failure and piercing failure. The proposed failure modes can be seen through the cross-section of mortar joint in Fig. 4.

3.2.1. Buckling failure

Buckling of the tie was found to be the most frequent failure mode in compression [4]. In order to determine the critical buckling load, the Euler formula was used as starting points; the equation was then revised in case of bent ties.

The compression strength is determined as the Euler's critical load as follows:

$$N = \frac{\pi^2 \times E \times I}{K^2 \times {l_c}^2} \tag{8}$$

where K is the column effective length factor, E is the elastic modulus of the tie, I is the second moment of area of the tie and l_c is the cavity length between two leaves. For bent ties, the compression strength can be computed as follows to take into account the initial deformation:

$$N = \frac{\pi^2 \times E \times I}{K^2 \times {l_c}^2} - \frac{12 \times E \times I \times \phi}{l_c \times d^3} \tag{9}$$

The factor K is chosen 0.5 for all the typologies due to the clamped–clamped boundary conditions of the tie provided by the embedment in the mortar joints.

3.2.2. Piercing failure (Bearing Failure)

The piercing failure is characterized by a portion of mortar punched out from beneath the cavity wall tie. The width of the piece of mortar is limited by the width of the embedded head of the tie, whereas the length corresponds to the length of the bent part of the tie. No mechanical model has been proposed in the literature to determine the piercing strength of a wall tie connection in a masonry wall. However, the phenomenon of mechanical behaviour of piercing in a masonry is developed by analogy of the bearing failure in concrete. Thus, the approach for computing the bearing strength in concrete can be used as starting point also for connections in masonry walls.

Hawkins [37] proposed a method for determining the bearing strength of concrete, which shows good agreement to predict the failure modes and loads in tested specimens. His model is based on a wedge theory, where the wedge, which forms under the bearing plate, splits the surrounding concrete. He assumed that the movement of the wedge is restrained by frictional forces and normal forces along the wedge. The piercing capacity of the cavity wall ties can be calculated according to an equation that is derived following the approach proposed by Hawkins (Eq. (10)):

$$\boldsymbol{N = A_1 \times (f_m + 12.5 \times f_t \times \left(\sqrt{\frac{A_2}{A_1}} - 1\right))} \tag{10}$$

with:

$$f_t = 0.332 \times \sqrt{f_m} \tag{11}$$

$$\boldsymbol{A_1 = l_h \times d} \tag{12}$$

$$\boldsymbol{A_2 = l_h \times c} \tag{13}$$

where f_t is the tensile strength of the mortar, A_1 is the area of the loaded end which is under either the hooked end or zigzag end, and A_2 is the piercing area of mortar under the loaded end. It should be noted that cohesion between the brick and mortar is neglected due to the relatively small failure area. The details of A_1 and A_2 can be seen in the drawing in Fig. 5. The expressions of l_h and d in Eq. (12) and Eq. (13) are chosen as the thickness of mortar for CB masonry due the zigzag shape of the tie.

3.2.3. Punching failure

Punching failure is characterized by the development of cracks from the end of the embedded tie and up to the face of the mortar joint, followed by the detachment of a conical body from the mortar joint.

The formulation proposed by the ACI code is based on an empirical relationship derived for punching in concrete [29]. Concrete is a material that is not directly comparable with mortar. It is, however, the closest material to mortar, from which, an analogy of behaviour can be derived. An idealized control perimeter 'u' at a distance 'c' from the end of the tie to the surface of the mortar is considered on the basis of the ACI code. The idealized control perimeter for a cavity wall tie can be seen in Fig. 6. Hence, the punching resistance of cavity wall ties can be determined as follows:

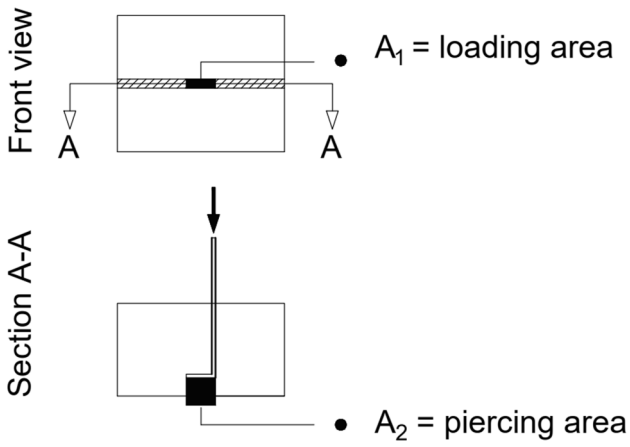

Fig. 5. The failure area of Piercing: front view (top) and mortar joint section (bottom).

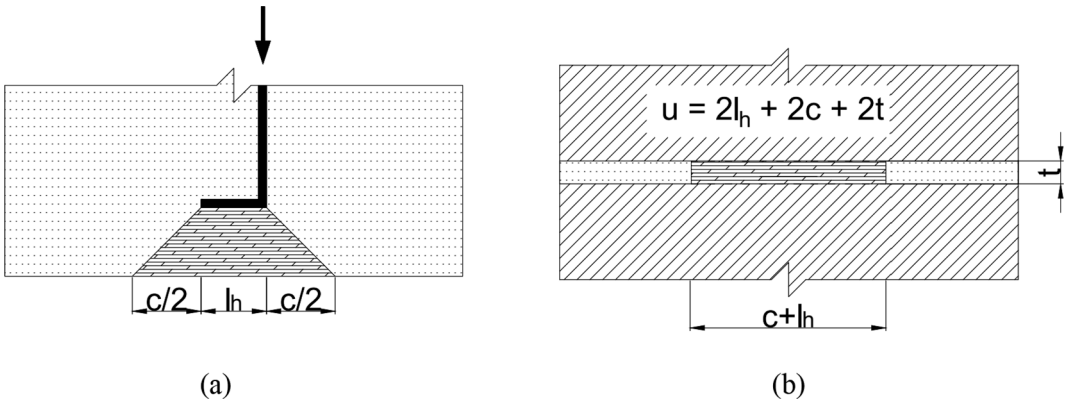

Fig. 6. Idealized control perimeter for cavity wall tie specimens for punching failure: mortar joint section (a), front view (b).

$N = 0.332 \times \sqrt{f_m} \times u \times c$

It is assumed that punching failure occurs when the normal stress determined by the force applied in compression reaches a critical value equal to $0.332 \times fm^{0.5}$ in MPa. Cohesion between the brick and mortar is neglected due to the relatively small failure area.

3.3. Calibration of the proposed model against the tests performed at TU Delft

The proposed mechanical model is calibrated against the experimental campaign conducted by the authors and completely reported in [4]. The campaign aimed to characterize the cyclic axial behaviour of metal cavity wall ties. Each specimen consisted of a couplet made of two bricks (either CS or clay bricks) connected by a 10 mm thick mortar joint, with a wall tie embedded in the joint. L-shaped ties with a diameter of 3.6 mm and a length of 200 mm were used between two bricks in the mortar joint. A total of 202 couplets were tested. Four types of specimens were tested:

- CS70: the hooked part of the tie is embedded in the CS leaf, with an anchoring length of 70 mm (Fig. 7a);
- CB50: the zigzag-end part of the tie is embedded in the CB leaf, with an anchoring length of 50 mm (Fig. 7b);
- CS50: the hooked part of the tie is embedded in the CS leaf, with a reduced embedment length of 50 mm (Fig. 7c);
- CS70-15D: the hooked part of the tie is embedded in the CS leaf, with an anchoring length of 70 mm; in addition, the zigzag-end of the tie is bent 15-degree (Fig. 7d).

The test setup was assembled based on the recommendations reported in EN-846–5 [39]. The specimen was placed in the setup with the tie aligned vertically along the centreline axis of the test machine, and the distance between the couplet and clamp was set equal to the standard cavity width (80 mm). Two different loading protocols were applied: quasi-static monotonic and cyclic loading. The cyclic loading protocol was composed by two phases: in the first phase groups of three cycles with the same amplitude were repeated, whereas in the second phase groups of two cycles were followed by two degradation cycles at lower amplitudes performed with the purpose of capturing the cyclic degradation on the tie-mortar bond. The amplitude of the cycles was defined based on the outcomes of the monotonic tests.

A set of companion tests was performed to determine the mechanical properties of the mortar used in the experiments: the flexural and compressive strength of the mortar was defined in agreement with NEN-EN 1015–11 [41], and the bond strength between masonry unit and mortar in agreement with NEN-EN 1052–5 [42]. In the experimental campaign, a cement-based mortar in the M5 strength class (nominal compressive strength 5 MPa) was used. The mechanical properties of the mortar resulting from the companion test are listed in Table 1. The capacity of the connections derived from the experimental campaign used for the calibration of the mechanical model are summarized in Table 2.

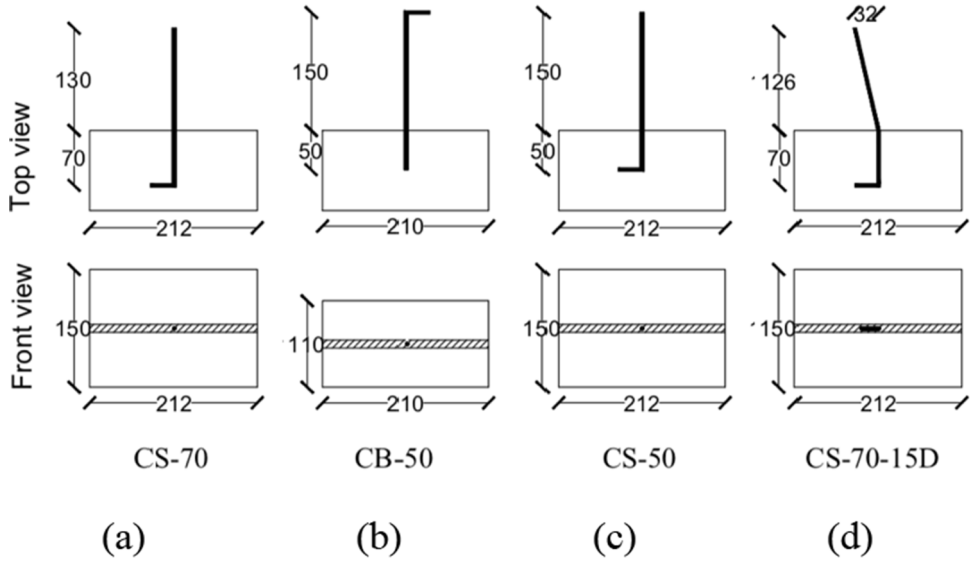

Fig. 7. Geometry of tie specimens [4]

Table 1
Mortar mechanical properties.

Material property	UM	CS Average	C.o. V.	CB Average	C.o. V.
Compressive strength of mortar	MPa	5.65	0.15	6.47	0.11
Flexural strength of mortar	MPa	2.43	0.14	2.29	0.24
Flexural bond strength	MPa	0.34	0.26	0.52	0.27

Table 2
Summary of cavity wall tie connection properties.

Material Characteristic	Unit	Symbol	Failure type	Typology CS70	CB50
Diameter of the tie	mm	d	Piercing Failure	3.6	10
			All	3.6	3.6
Tensile Strength of the tie	MPa	f_u	All	411	411
Compressive strength of the mortar	MPa	f_m	All	5.65	6.47
Tie embedment length	MPa	l_b	All	70	50
Joint thickness	mm	t	All	10	10
Friction coefficient of Mortar	–	μ	All	0.81	0.66
Initial shear strength of mortar	MPa	f_{v0}	All	0.24	0.82
Selected precompression level	MPa	f_p	All	0.1	0.1
Based thickness of the tie	mm	l_h	Pull-out Failure	25	0
			Piercing Failure	25	10
			Punching Failure	25	7.2
Edge distance	mm	c	All	30	50
Modification factor	–	α	All	0.5	1
Elastic modulus of the tie	MPa	E	All	32,920	32,920
Cavity length	mm	l_c	All	80	80

The couplets subjected to monotonic tensile loading exhibited either of the following failure modes: (a) pull-out failure, characterized by sliding the tie along the tie-mortar interface, or (b) tie failure, with first yielding and then fracture of the tie. Regarding the compressive loading, the couplets showed either of the failure modes: (c) buckling of the tie, or (d) expulsion failure, achieved by piercing and expulsion of the cone of mortar around the tie. The cyclic tests returned in tension and compression a combination of the four failure mechanisms described above for the monotonic loading. Fig. 8 shows the observed failure mechanisms from the experimental campaign.

The values of the capacity predicted via the proposed mechanical model are compared to the experimental results in terms of force capacity by grouping the results per type of connection and loading (monotonic and cyclic), as shown in Table 3.

In the experimental campaign conducted by the authors [4], it was found that the embedment length and the geometry of the tie affect significantly the capacity of the connection, while the applied precompression does not have a significant impact. Since the outcomes of the experiment tests are not affected by the four levels of precompression applied (0 MPa, 0.1 MPa, 0.3 MPa, and 0.6 MPa), this variation is hereinafter not considered.

As shown in Table 3, there are some cases for which the experimental failure does not always correspond to the lowest predicted capacity. The unexpected results of the model can be summarized as follow:

- The failure mode of CS70, CS50, CS70-15D in tension, and CB-50, CS50, CS70-15D in compression is correctly predicted.
- Regarding CS70 in compression, two different failure modes were observed during the experiment. The model predicts the most frequent failure mode (buckling) correctly as the lowest predicted capacity. In contrast, the experimental capacity for piercing obtained in case of this failure mode is lower than the one indicated by the proposed model. The observed piercing capacity was low in the experimental campaign because the straightening of the hooked end of the tie resulted in a smaller load bearing area of the head.
- Regarding CB50 in tension, there were two different observed failure modes from the experiment, namely tie failure and pull-out failure. The values predicted by the model are close to the strength measured at failure for both modes. However, in few cases, the specimens had larger pull-out strength possibly due to unexpected interlocking between tie and mortar, determining eventually the failure of the tie in place of the pull-out failure (which is predicted by the proposed model as the lowest capacity).

Pull-out failure under tension and buckling under compressive loading are the most common failure modes observed during the experimental campaign: 92% of the specimens undergo pull-out failure in tension and 92% buckling failure in compression. The predictions obtained with the proposed model agree satisfactorily with the experimental results. Also the mean peak force is computed with adequate accuracy: as shown in Fig. 9, the error between the experimental results and the proposed mechanical model for the pull-out and buckling failure is never larger than 13% for monotonic loading and 11% for cyclic loading. The error is computed as the difference between the mean experimental result and the proposed mechanical model divided by the mean experimental result. The error can be calculated by using Eq. (15):

$$error = \frac{N_p - N_e}{N_e} \tag{15}$$

where N_e is the mean experimental result and N_p is the result from the proposed mechanical model. As shown in Fig. 9, in the underperformed part, the brackets indicate the number of specimens that are below the predicted value of the proposed model compared to the total number of specimens tested for each corresponding variation. Conversely, the bracket shows the number of specimens above the predicted value for each corresponding variation in the outperformed part.

4. Extension of the model to untested configurations

The experimental campaign conducted by the authors on cavity wall ties considered a large number of variations which were seen in common construction practice, such as two different embedment lengths, two different tie geometries, four pre-compression levels, and five different testing protocols. More parameters can influence the behaviour of the cavity wall tie connections, but it is impractical to conduct an experimental campaign considering all the possible influence parameters. Hence, a consistent sensitivity study of the key parameters was performed making use of the proposed mechanical model. The following additional variations of the parameters are considered: (i) a different (15 MPa) mortar strength for CS couplets, (ii) a shorter (60 mm) cavity depth, (iii) a different (70 mm) embedment depth for CB walls and (iv) solid brick for CB. All the studied parameters are summarized in Table 4. The parameters described below are varied individually.

4.1. Mortar with higher strength class

The majority of the masonry buildings in the Netherlands were mainly made of low-quality mortar [43]. For the parametric study, a higher mortar strength (15 MPa) is chosen for the CS specimens . Fig. 10 shows how the strength of the connection is predicted to change for each failure mode and for each specimen type when the new higher value of the mortar strength is considered. As expected, an increase in the mortar strength leads to an increase of break-out, pull-out, punching and

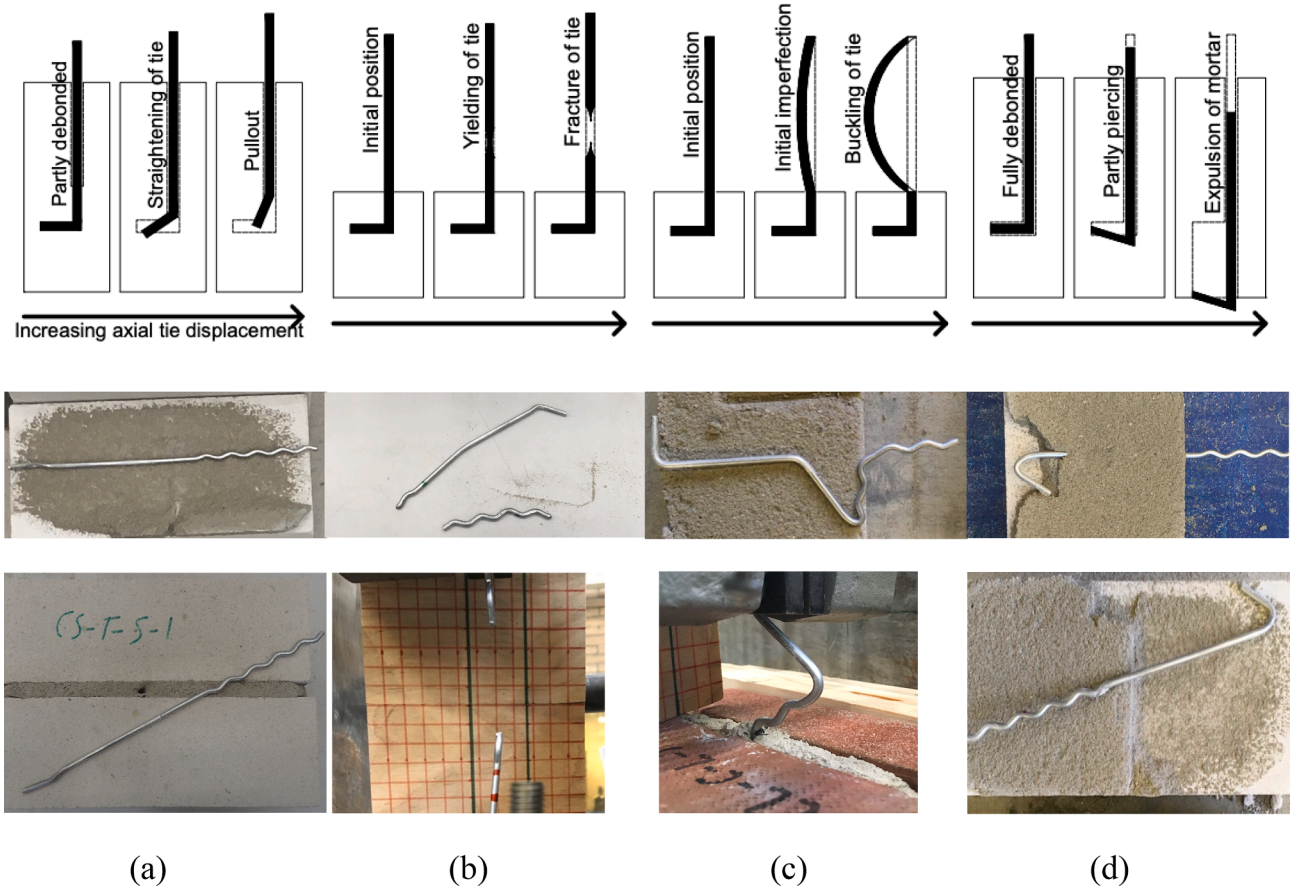

Fig. 8. Failure mode sequence: Pull-out failure (a), Tie failure (b), Buckling failure (c) and expulsion failure [4].

Table 3
Predicted and average experimental failure modes and capacities of the tested wall tie connections.

Typology		TieFailure	Cone Break-outFailure	Pull-outFailure	BucklingFailure	PunchingFailure	PiercingFailure
CS70	**Proposed Model**	4.18	4.25	2.04	1.69	3.09	2.17
	Experiment(Mono)	–	–	2.35	1.83	–	1.51
	Experiment (Cyclic)	–	–	1.88	1.78	–	1.63
CB50	**Proposed Model**	4.18	5.28	3.19	1.69	5.70	1.94
	Experiment(Mono)	4.22	–	3.43	1.83	–	–
	Experiment (Cyclic)	3.95	–	3.32	1.60	–	–
CS50	**Proposed Model**	4.18	2.40	1.77	1.69	6.73	2.91
	Experiment(Mono)	–	–	1.87	1.80	–	–
	Experiment (Cyclic)	–	–	1.62	1.90	–	–
CS70-15D	**Proposed Model**	4.18	4.25	2.27	1.42	3.09	2.17
	Experiment(Mono)	–	–	2.51	1.35	–	–
	Experiment (Cyclic)	–	–	2.07	1.44	–	–

piercing strength. On the other hand, the increase in the mortar strength does not influence the buckling capacity or the steel rupture failure. As a consequence, the use of stronger mortar leads to more frequent steel rupture failure in tension and buckling failure in compression.

4.2. Reduced cavity width

A cavity width of 60 mm is considered in alternative to the more usual value of 80 mm, to consider potential errors and inaccuracies in the construction practice. Fig. 11 shows the variation of the predicted strength for each failure mode and each specimen type. It is noted that the predicted strength for the cavity width of 60 mm is conducted without changing other parameters such as the embedment length of CB or CS.

A change in the cavity width affects only the buckling capacity of the ties in compression since a decrease in the gap of between the two leaves leads to an increase in the buckling capacity (Fig. 11). Therefore, a reduced width of the cavity may affect the governed failure mode in compression.

4.2.1. Longer embedment depth for CB

In the experimental campaign conducted by the authors, the CS specimens were investigated under two different embedment depths (50 mm or 70 mm), but only a length of 50 mm was considered for the embedment of the ties in the CB specimens. In this section, the effects of an increased embedment length of 70 mm in CB walls (which may be due to an imperfect application) are evaluated.

An increase in the embedment depth in the CB specimens determines higher strength capacity in cone break-out and pull-out failure and a lower strength for punching and piercing failure (Fig. 12).

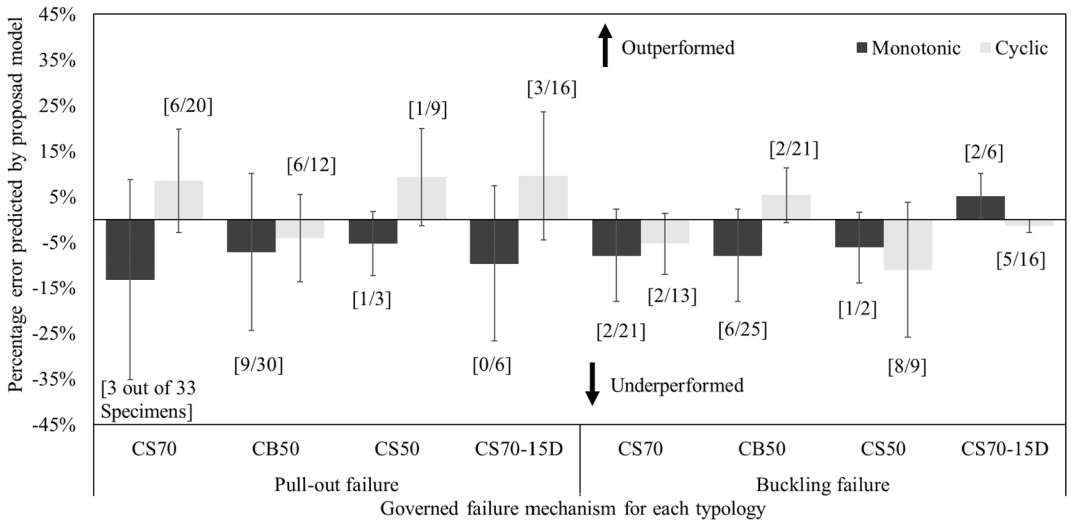

Fig. 9. Error for the predicted values using the proposed mechanical model versus the experimental data. Error bars indicate standard deviation.

Table 4
The studied parameters for the extension of the proposed model.

Type	Mortar Strength		Embedment depth		Type of Brick		Cavity width
	CB Leave	CS Leave	CB Leave	CS Leave	CB Leave	CS Leave	
Tested combination	M5	M5	50 mm	70 mm	PerforatedCB brick	CS	70 mm
P1 – 15 MPaCS mortar	M5	M15	50 mm	70 mm	PerforatedCB brick	CS	70 mm
P2 – 60 mmCavity width	M5	M5	50 mm	70 mm	PerforatedCB brick	CS	60 mm
P3 – 70 mmembedded CB	M5	M5	70 mm	50 mm	PerforatedCB brick	CS	70 mm
P4 – SolidClay Brick	M5	M5	50 mm	70 mm	SolidCB brick	CS	70 mm

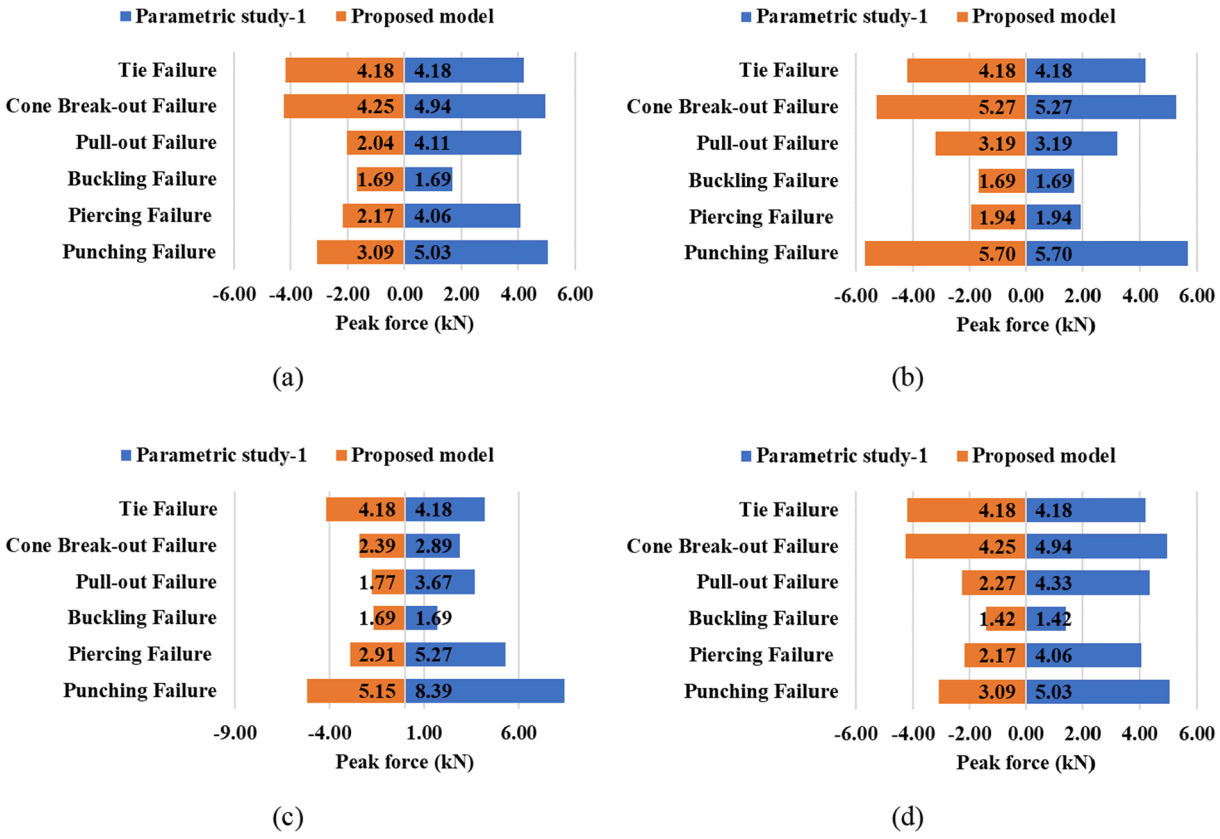

Fig. 10. Comparison between the proposed model and the parametric study-1 :CS70 (a), CB50 (b), CS50 (c) and CS70-15D (d).

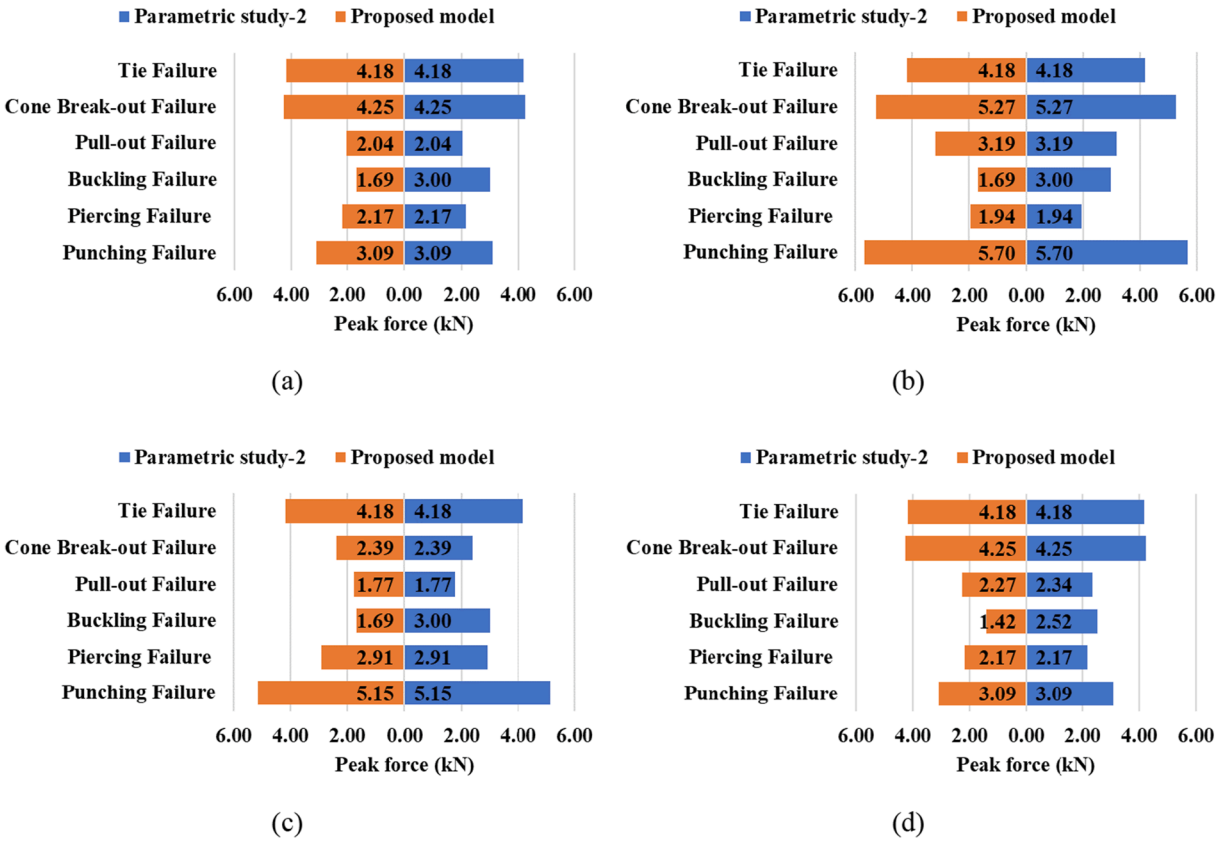

Fig. 11. Comparison between the proposed model and the parametric study-2 :CS70 (a), CB50 (b), CS50 (c) and CS70-15D (d).

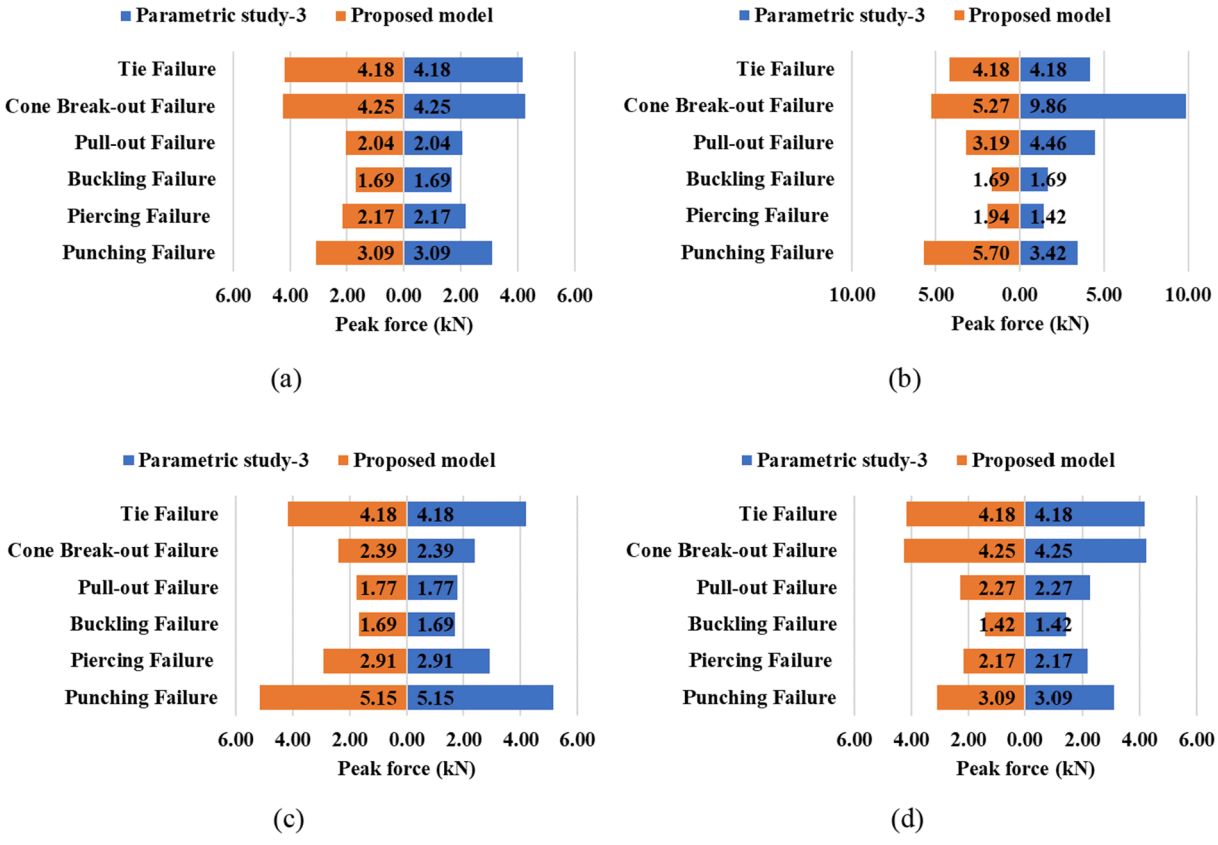

Fig. 12. Comparison between the proposed model and the parametric study-3: CS70 (a), CB50 (b), CS50 (c) and CS70-15D (d).

4.3. Solid clay bricks

For the experimental campaign carried out by the authors, perforated bricks were used for the clay masonry outer leave. In addition, the embedment in solid clay brick masonry for cavity walls is conducted to provide a better representative result for cavity walls. Jafari et al. [38] provides the initial shear parameters, including initial shear strength and coefficient of friction for the solid brick for CB specimens which are employed for the parametric study. A comparison between the proposed model and the studied parameter is shown in Fig. 13. Due to the absence of the dowel affect, cone breakout failure is more likely to be observed.

4.4. Summary of the failure modes for all the different configurations studies

A summary of the results obtained via the parametric study is reported in Fig. 14 and Table 5. Overall, the parametric analysis showed that the governed failure mode, marked in bold letters in Table 5, can change due to the variation of the parameters, as expected. Nevertheless, the most frequent failure modes remain pull-out under tension and buckling in compression. A different mortar strength for CS couplets affects the failure mode due to the development of a more efficient bonding between the mortar and tie in tension, while it does not have influence in compression since the buckling failure is governing. Due to the shorter cavity depth, which leads to an increasing of the buckling strength, the failure mechanism changes to piercing failure. A different embedment depth for CB walls may change the governing failure mode in both tension and compression due to the reduced distance to the edge, so that the connection may be vulnerable to piercing failure. Finally, the use of solid clay bricks does not have a significant influence on the governing failure mode, neither in tension nor in compression.

5. Conclusions

This paper aims at developing a mechanical model to predict the failure mode and the strength capacity of metal tie connections in masonry cavity walls. The paper investigates connections embedded in double-leaf cavity walls composed of an inner load-bearing leaf made of calcium silicate brick masonry and an outer leaf made of clay brick masonry, which are very common in the province of Groningen in the north of the Netherlands.

The model considers six possible failure modes, which are tie failure, cone break-out failure, pull-out failure, buckling failure, punching failure and piercing failure. The prediction of one of these failure modes is based on the characteristics of the used materials, type of the bricks and ties, embedment length, mortar quality, etc. A good agreement between the experiments conducted by the authors and the proposed model is found in terms of both identification of the failure mode and determination of the peak capacity of the connection.

The following results are reported:

- The proposed mechanical model is capable of predicting the failure modes observed during the experimental campaign, which are pull-out and buckling failure. However, it should be noted that two different failure modes were observed regarding CS70 in compression and CB50 in tension from the experiment. As mentioned before, the model predicts correctly the most frequent failure mode.
- The model accurately predicts the strength capacity of the cavity wall ties. The ratio between the experimental results and mechanical model ($N_{Test}/N_{Predicted}$) for pull-out and buckling failure are determined as 1.04 and 1.04 with standard deviations of 0.15 and 0.10, respectively.
- The parametric analysis showed that the studied parameters, which are mortar with higher strength, reduced cavity width, longer embedment depth and a different type of brick, moderately influence

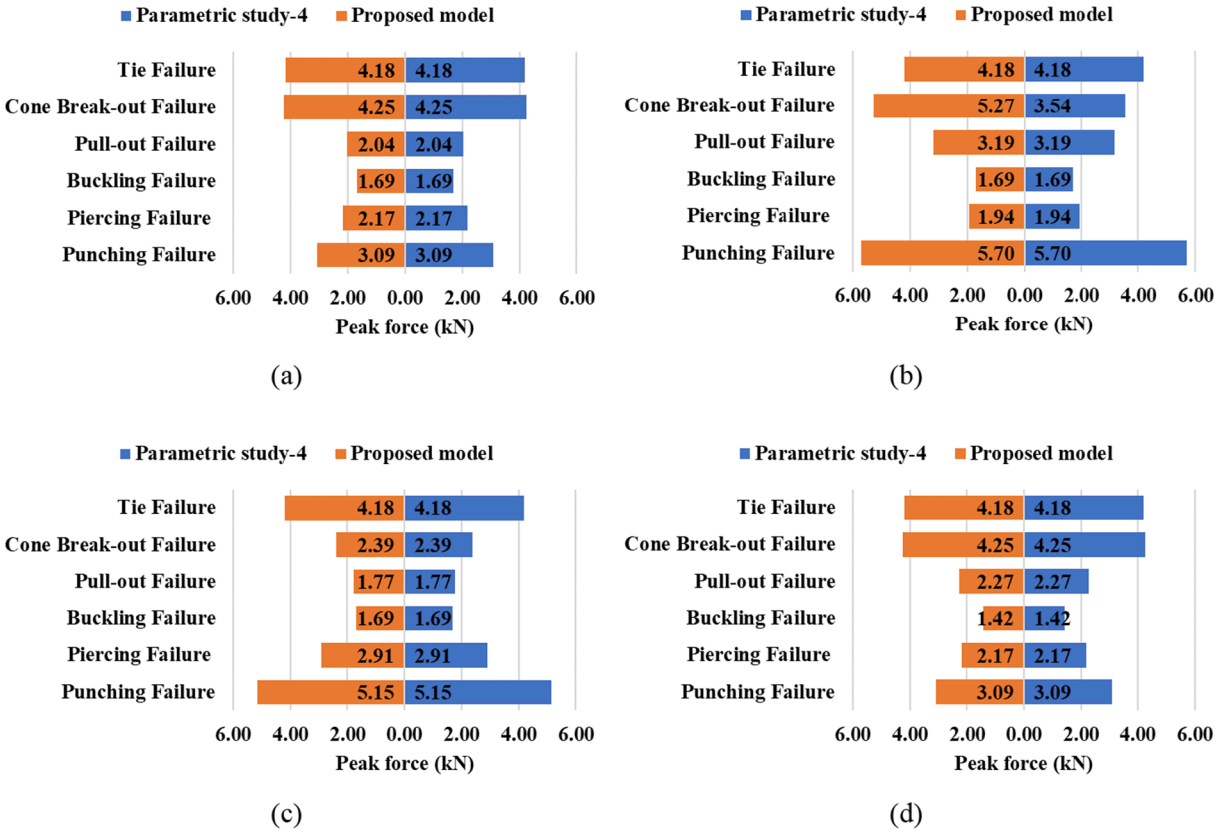

Fig. 13. Comparison between the proposed model and the parametric study-4: CS70 (a), CB50 (b), CS50 (c) and CS70-15D (d).

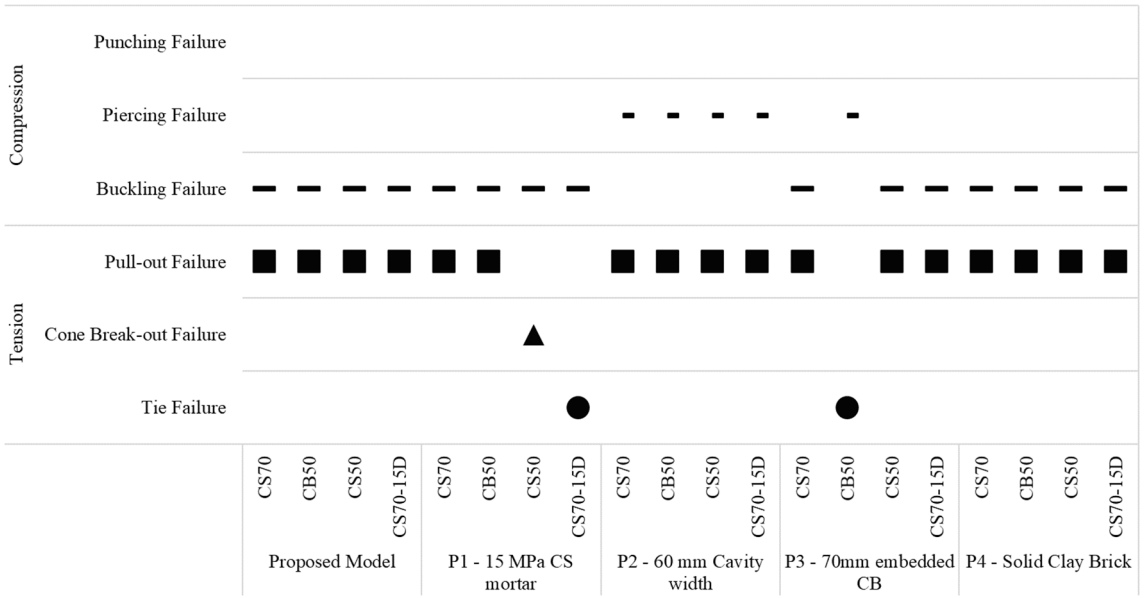

Fig. 14. Governed failure modes for parametric study.

Table 5
Obtained results by parametric study (the governed failure mode marked in bold letters).

Parametric study	Typology	Tension TieFailure (kN)	ConeBreak-outFailure (kN)	Pull-outFailure (kN)	Compression BucklingFailure (kN)	PiercingFailure (kN)	PunchingFailure (kN)
P1-15 MPa CS mortar	CS70	4.18	4.94	**4.11**	**−1.69**	−4.06	−5.03
	CB50	4.18	5.27	**3.19**	**−1.69**	−1.94	−5.70
	CS50	4.18	**2.89**	3.67	**−1.69**	−5.27	−10.97
	CS70-15D	**4.18**	4.94	4.33	**−1.42**	−4.06	−5.03
P2-60 mm Cavity width	CS70	4.18	4.25	**2.04**	−3.00	**−2.17**	−3.09
	CB50	4.18	5.27	**3.19**	−3.00	**−1.94**	−5.70
	CS50	4.18	2.39	**1.77**	−3.00	**−2.91**	−6.73
	CS70-15D	4.18	4.25	**2.34**	−2.52	**−2.17**	−3.09
P3-70 mm embedded CB	CS70	4.18	4.25	**2.04**	**−1.69**	−2.17	−3.09
	CB50	**4.18**	9.86	4.46	−1.69	**−1.42**	−3.42
	CS50	4.18	2.39	**1.77**	**−1.69**	−2.91	−6.73
	CS70-15D	4.18	4.25	**2.27**	**−1.42**	−2.17	−3.09
P4-Solid Clay Brick	CS70	4.18	4.25	**2.04**	**−1.69**	−2.17	−3.09
	CB50	4.18	3.54	**3.19**	**−1.69**	−1.94	−5.70
	CS50	4.18	2.39	**1.77**	**−1.69**	−2.91	−6.73
	CS70-15D	4.18	4.25	**2.27**	**−1.42**	−2.17	−3.09

the failure type and the corresponding capacity of metal tie connections between the leaves in a cavity wall. A higher mortar strength has an impact on the tensile behaviour of the connection as it increases the bond between the mortar and the tie; conversely, for compression the failure mode is not affected by the mortar strength since the governing failure mode depends exclusively on the properties of the metal tie. A decrease in the cavity width increases the critical buckling load, leading to a different failure mode in compression; however, in tension the strength capacity of the metal tie connection does not change.

The authors believe that the presented model can be adopted by structural engineers to estimate the peak force capacity of wall tie connections and to assess the performance of such connections during seismic events in masonry cavity walls with the characteristic considered, whereas other constructive techniques and/or materials would require specific studies. The presented mechanical model can also be used as a basis for a constitutive model in finite element analysis. For this purpose, a hysteretic model can be employed, as obtained from the experimental campaign conducted by the authors [4], for the nonlinear force–deformation behaviour of the wall metal tie connection.

CRediT authorship contribution statement

O. Arslan: Writing – original draft. **F. Messali:** Supervision, Writing – review & editing. **E. Smyrou:** Supervision, Writing – review & editing. **İ.E. Bal:** Supervision, Writing – review & editing. **J.G. Rots:** Supervision, Writing – review & editing.

Declaration of Competing Interest

The authors declare that they have no known competing financial interests or personal relationships that could have appeared to influence the work reported in this paper.

References

[1] R.G. Drysdale, A.A. Hamid, L.R. Baker, Masonry structures : behavior and design, Englewood Cliffs, N.J: Prentice Hall, 1994.

[2] H.O. Sugo, A.W. Page, B. Moghtaderi, A comparative study of the thermal performance of cavity and brick veneer construction, 13th Int. Brick Block Mason. Conf. - IBMAC. (2004) 767–776.

[3] H. Derakhshan, W. Lucas, P. Visintin, M.C. Griffith, Out-of-plane Strength of Existing Two-way Spanning Solid and Cavity Unreinforced Masonry Walls, Structures. 13 (2018) 88–101, https://doi.org/10.1016/j.istruc.2017.11.002.

[4] O. Arslan, F. Messali, E. Smyrou, İ.E. Bal, J.G. Rots, Experimental characterization of the axial behavior of traditional masonry wall metal tie connections in cavity walls, Constr. Build. Mater. 266 (2021) 121141, https://doi.org/10.1016/j.conbuildmat.2020.121141.

[5] S. Mertens, A. Smits, Y. Grégoire, Experimental parametric study on the performance of wall ties, Int. Mason. Conf. 2014 (2014) 1–11.

[6] N.V. Zisi, R.M. Bennett, Shear Behavior of Corrugated Tie Connections in Anchored Brick Veneer-Wood Frame Wall Systems, J. Mater. Civ. Eng. 23 (2) (2011) 120–130, https://doi.org/10.1061/(ASCE)MT.1943-5533.0000143.

[7] Y.-H. Choi, J.M. LaFave, Performance of Corrugated Metal Ties for Brick Veneer Wall Systems, J. Mater. Civ. Eng. 16 (3) (2004) 202–211, https://doi.org/10.1061/(ASCE)0899-1561(2004)16:3(202).

[8] A. Martins, G. Vasconcelos, A.C. Costa, Experimental study on the mechanical performance of steel ties for brick masonry veneers (2016) 1723–1731.

[9] D. Reneckis, J.M. LaFave, Analysis of brick veneer walls on wood frame construction subjected to out-of-plane loads, Constr. Build. Mater. 19 (6) (2005) 430–447, https://doi.org/10.1016/j.conbuildmat.2004.08.006.

[10] V.P. Paton-Cole, E.F. Gad, C. Clifton, N.T.K. Lam, C. Davies, S. Hicks, Out-of-plane performance of a brick veneer steel-framed house subjected to seismic loads, Constr. Build. Mater. 28 (1) (2012) 779–790, https://doi.org/10.1016/j.conbuildmat.2011.10.033.

[11] D. Reneckis, J.M. LaFave, Out-of-plane seismic performance and detailing of brick veneer walls, J. Struct. Eng. 136 (7) (2010) 781–794, https://doi.org/10.1061/(ASCE)ST.1943-541X.0000169.

[12] D. Reneckis, J.M. LaFave, W.M. Clarke, Out-of-plane performance of brick veneer walls on wood frame construction, Eng. Struct. 26 (8) (2004) 1027–1042, https://doi.org/10.1016/j.engstruct.2004.02.013.

[13] W.M. McGinley, S. Hamoush, Seismic masonry veneer: quazi-static testing of wood stud backed clay masonry veneer walls, Proc. 2008 Struct. Congr. - Struct. Congr. 2008 Crossing Borders. 314 (2008). https://doi.org/10.1061/41016(314)220.

[14] M. Hatzinikolas, J. Longworth, J. Warwaruk, Strength and behaviour of anchor bolts embedded in concrete masonry, Alberta Masonry Institute, [Edmonton] (1979).

[15] R.H. Brown, A.R. Whitlock, Strength of Anchor Bolts in Grouted Concrete Masonry, J. Struct. Eng. 109 (6) (1983) 1362–1374, https://doi.org/10.1061/(ASCE)0733-9445(1983)109:6(1362).

[16] J.B. Tubbs, D.G. Pollock, D.I. McLean, Testing of anchor bolts in concrete block masonry, Mason. Soc. J. 18 (2000) 81/92.

[17] W.M. Mcginley, S. Singleton, J. Greenwald, J. Thompson, CAPACITY OF ANCHOR BOLTS IN CONCRETE MASONRY, 2004.

[18] H. Krenchel, S.P. Shah, Fracture analysis of the pullout test, Mater. Struct. 18 (6) (1985) 439–446, https://doi.org/10.1007/BF02498746.

[19] G. Rehm, J. Schlaich, K. Schäfer, R. Eligehausen, Fritz-Leonhardt-Kolloquium 1984. 15. Forschungskolloquium des Deutschen Ausschusses für Stahlbeton (Teil 1)., Beton- Und Stahlbetonbau. 80 (1985). https://doi.org/10.1002/best.198500310.

[20] H. Bode, K. Roik, Headed Studs-Embedded in Concrete and Loaded in Tension, Spec. Publ. 103 (1987) 61–88. https://doi.org/10.14359/1671.

[21] G. Rehm, R. Eligehausen, R. Mallée, Befestigungstechnik : Sonderdruck aus dem Beton-Kalender 1992 (1991). https://doi.org/10.18419/opus-657.

[22] W. Fuchs, R. Eligehausen, J.E. Breen, Concrete Capacity Design (CCD) Approach for Fastening to Concrete, Authors' Closure to Discussions, ACI Struct. J. 92 (1995) 794–802.

[23] W. Fuchs, R. Eligehausen, Das CC-Verfahren für die Berechnung der Betonausbruchlast von Verankerungen, Beton- Und Stahlbetonbau. 90 (1) (1995) 6–9, https://doi.org/10.1002/best.v90.110.1002/best.199500020.

[24] F. Arifovic, M.P. Nielsen, Strength of anchors in masonry, Byg Rapport No (2006) R-134.

[25] L.Z. Hansen, K. Findsen, M.P. Nielsen, Beregning af indlimede ankre i murede vaegge, 2004. http://www.byg.dtu.dk/publications/rapporter/byg-.

[26] M.P. Nielsen, L.C. Hoang, Limit analysis and concrete plasticity, 2016.

[27] MSJC, Building Code Requirements and Specification for Masonry Structures, Mason. Stand. Jt. Comm. (2013).

[28] J. Moe, Shearing strength of reinforced concrete slabs and footings under concentrated loads, Portl. Cem, Assoc, 1961.

[29] ACI Committee 318, Commentary on Building Code Requirements for Structural Concrete (ACI 318R-19), Am. Concr. Inst. (2019).

[30] E.A. Toubia, J. Lintz, In-Plane Loading of Brick Veneer over Wood Shear Walls, Mason. Soc. J. 31 (2013).

[31] Australian Standard., AS 3700-2018: Masonry Structures, (2018).

[32] A.W. Page, J. Kautto, P.W. Kleeman, A Design Procedure for Cavity and Veneer Wall Ties, (1996).

[33] A.W. Page, G. Simundic, M. Masia, A Study of Wall Tie Force Distribution in Veneer Wall, J. Ind. Econ.LV (2007) 0022–1821.

[34] K. Høiseth, A.M.Y. Hamed, T. Kvande, Evaluation of Seismic Code Regulations on Typical Veneer Walls, Int. Mason. Conf. 2014 (2014) 1–10.

[35] A. Martins, G. Vasconcelos, A. Campos Costa, Experimental study on the mechanical performance of steel ties for brick masonry veneers, Brick Block Mason. Trends, Innov. Challenges - Proc. 16th Int. Brick Block Mason. Conf. IBMAC 2016. (2016) 1723–1732. https://doi.org/10.1201/b21889-214.

[36] D.P. Kuhn, F.A. Shaikh, Slip-Pullout Strength of Hooked Anchors, Res, Univ. Wisconsin-Milwaukee, Submitt. to Natl. Codes Stand. Counc, Report, 1996.

[37] N.M. Hawkins, The bearing strength of concrete loaded through rigid plates, Mag. Concr. Res. 21 (1969) 225–227, https://doi.org/10.1680/macr.1969.21.69.225.

[38] S. Jafari, J.G. Rots, R. Esposito, F. Messali, Characterizing the Material Properties of Dutch Unreinforced Masonry, Procedia Eng. 193 (2017) 250–257, https://doi.org/10.1016/j.proeng.2017.06.211.

[39] Nederlands Normalisatie-instituit (NEN)., NEN-EN 846-5: Methods of test for ancillary components for masonry - Part 5: Determination of tensile and compressive load capacity and load displacement characteristics of wall ties (couplet test), (2010).

[41] Nederlands Normalisatie-instituit (NEN), NEN-EN 1015-11: Methods of test for mortar for masonry - Part 11: Determination of flexural and compressive strength of hardened mortar, (1999).

[42] Nederlands Normalisatie-instituit (NEN), Nen-en 1052-5: Methods of test for masonry - Part 5: Determination of bond strength by the bond wrench method, (2005).

[43] Eucentre, P&P, TU Delft, TU Eindhoven, Material Characterization, Groningen Earthquakes – Struct. Upgrad. Mater. Charact. – Version 1.4. (2015).